Capillary Stress and Structural Relaxation in Moist Granular Materials

Tingtao Zhou,[*,†] Katerina Ioannidou,[*,‡,‖] Enrico Masoero,[*,¶] Mohammad Mirzadeh,[*,§] Roland J.-M. Pellenq,[*,‡,‖] and Martin Z. Bazant[*,§,#]

†*Massachusetts Institute of Technology, Department of Physics*

‡*MultiScale Materials Science for Energy and Environment (MSE2), The Joint CNRS-MIT-Aix-Marseille University Laboratory, UMI CNRS 3466, Massachusetts Institute of Technology, Cambridge, Massachusetts 02139, USA*

¶*Newcastle University, School of Engineering, United Kingdom*

§*Massachusetts Institute of Technology, Department of Chemical Engineering*

‖*Department of Civil and Environmental Engineering, Massachusetts Institute of Technology, Cambridge, Massachusetts 02139, USA*

⊥*Massachusetts Institute of Technology, Department of Mathematics*

#*Mailing Address: 77 Massachusetts Avenue, Cambridge, MA, 02139, USA.*

E-mail: tingtaoz@mit.edu; hekate@mit.edu; enrico.masoero@newcastle.ac.uk; mirzadeh@mit.edu; pellenq@mit.edu; bazant@mit.edu

Abstract

A numerical and theoretical framework to address poromechanical effect of capillary stress in complex mesoporous materials is proposed and exemplified for water sorption in cement. We first predict the capillary condensation/evaporation isotherm using lattice-gas simulations in a realistic nano-granular cement model. A phase-field model to calculate moisture-induced capillary stress is then introduced and applied to cement

at different water content. We show that capillary stress is an effective mechanism for eigenstress relaxation in granular heterogeneous porous media, which contributes to the durability of cement.

Keywords

capillary condensation, wet granular materials, stress relaxation, cement paste, poromechanics

Introduction

Capillary condensation is a ubiquitous process of vapor-liquid phase transition in porous media, such as sand piles, plaster, paints, silica gels, cementitious materials, which has an important yet poorly understood effect on mechanical behavior. The confined fluid can generate enormous local stresses, as observed in granular material aging[1], wet floor friction[2], nano-tribology[3], multi-phase immiscible flows[4,5], cement drying shrinkage[6,7] and in everyday life experiences such as hardening of a drying sponge or building a sand castle on the beach[8]. Capillary condensation and evaporation potentially bring undesirable fracture processes, as in drying cracking of colloidal films[9,10] and paints[11], but capillary stress can also can be exploited in nano-materials fabrication by capillary force lithography[12], capillary rise infiltration,[13,14] evaporation-driven assembly and self-organization[15–18] and composite imbibition[19] and even used to evaluate the atmosphere of planets[20].

Despite the broad importance of capillary forces, they remain challenging to predict in complex porous materials over the full range of liquid saturation, either in equilibrium or during a dynamical process of drainage/imbibition. For granular or colloidal materials, existing models addressing partial saturations are oversimplified and only apply either to low humidity (so called pendular/funicular regimes)[21–23] or to idealized geometries (slit/cylindrical independent pores or single sphere against a wall)[24–27]. At higher saturation, models based

on geometrical analysis of Young-Laplace equation for smaller clusters[28,29] are proposed but restricted to only equilibrium liquid distributions inside monodisperse packings. A full molecular treatment here is beyond current computational capability, since that will require considering hundreds of millions of water molecules for our system.

Structural changes due to adsorption/desorption in porous media are known as "sorption induced deformation". We refer the reader to Gor et al[30] for a review on the topic. We also refer the readers to the recent work of Schappert et al[31] reporting the poromechanics of Vycor, a porous silica glass, upon argon sorption. In this work, an unexpected sharp contraction followed by re-expansion was observed upon desorption. Notice that here we are concerned with capillary stress induced deformation only, therefore surface effects (Bangham effect[32]) that might occur at low relative humidity are beyond the scope of this work.

In this Article, we propose a numerical and theoretical framework to quantitatively predict capillary condensation/evaporation[33,34], compute associated capillary forces and structural relaxation in a 3D realistic nano-granular cement paste model[35] using lattice-gas simulations of adsorbed water[36] parametrized from atomistic simulations[37]. In particular, this allowed us to access the adsorption/desorption mechanism and assess the role of (metastable) cavitation[38]. In addition, we present for the first time to our knowledge a phase-field model of the liquid-vapor mixture spatial distribution, whose inhomogeneous stress tensor is integrated over Voronoi polyhedra in order to calculate forces between each pair of neighboring grains. The capillary forces applied to the cement hydrate nano-grains in molecular dynamics (MD) simulations, together with the cohesive interactions between these nano-grains predict the overall stress relaxation. As an important application, we calculate drying shrinkage of cement paste[6,39–41], where the heterogeneous and multi-scale, fully connected porous network induces significant mechanical irreversibilities during drying-wetting cycles[42], disqualifying simple models based on macroscopic homogenized poromechanics concepts, hence ignoring local heterogeneities in the pore voids and solid-fluid interactions.

Methods

Capillary condensation/evaporation isotherm— We simulated capillary condensation and evaporation processes in our previously developed realistic mesoscale model of cement paste[35], using a discrete lattice gas density functional theory (DFT) with interaction parameters imported from water/cement atomistic simulations[37]. This DFT approach was first derived by Kierlik et al[36,43] for adsorption/desorption of a fluid in a quenched random porous solid. This method has been further applied to Vycor[44], controlled porous silica glasses and aerogels[45,46] to infer qualitatively adsorption/desorption isotherms through the minimization of the grand potential:

$$\begin{aligned}\Omega = & - w_{ff} \sum_{<i,j>} \rho_i \rho_j - w_{sf} \sum_{i,j} \rho_i \eta_j - \mu \sum_i \rho_i \\ & + k_B T \sum_i \left[\rho_i \ln \rho_i + (1 - \rho_i) \ln(1 - \rho_i) \right]\end{aligned} \tag{1}$$

where ρ_i, the normalized density of fluid on site i, can continuously vary from 0 to 1, $\eta_i = 0$ or $\eta_i = 1$ indicating site i is occupied by solid or not. w_{ff} and w_{sf} are the fluid-fluid interaction and fluid-solid interaction respectively that are imported from atomistic simulation data [37]. The cement paste porous structures used here comes from the out-of-equilibrium precipitation of cohesive interactions of calcium silicate hydrate (C-S-H) nanograins and has a realistic pore size distribution (gel pores and capillary pores below and above 3 nm respectively) and connectivity[35] (see SI). They have volume fraction 0.52 that corresponds to cement paste made with water to cement ratio (w/c) 0.45[47]. The lattice spacing a of our DFT simulation is estimated from the surface tension that is energy per area $\gamma \sim w_{ff}/2a^2$ for nitrogen at $T = 77$ K, $\gamma \sim 8.94$ mN/m which gives $a \sim 0.345$ nm; for water at $T = 300$ K, $\gamma \sim 72$ mN/m which gives $a \sim 0.24$ nm. Based on these estimates, we choose a fine grid cell size of $a = 0.3$ nm i.e close to molecular size. The fluid-fluid interaction w_{ff} is determined by the bulk critical point $k_B T_c = -\nu w_{ff}/2$ where ν ($\nu = 6$) is the number of nearest neighbors on the cubic lattice. The fluid-solid interaction $w_{sf} = 2.5\ w_{ff}$ is estimated

from molecular simulations of the isosteric heat of adsorption in the limit of zero coverage for water in cement paste[37].

Adopting the relation between chemical potential and relative saturating pressure h (or relative humidity in the case of water) $\mu = k_B T \ln(h)$, we show in Fig. 1a that the lattice DFT method with appropriate grid fineness is able to quantitatively predict the room temperature hysteretic water adsorption/desorption isotherm in cement paste in agreement with experiments[6,33,48,49] with no adjustable parameter. In particular the closure point of the hysteresis loop ($h \sim 30\%$) in the simulated isotherms is that observed in many water adsorption experiments at room temperature in disordered mesoporous materials[50].

There are many studies on water sorption in hardened cement paste reporting low pressure hysteresis loop in the adsorption/desorption isotherm[39,49]. This feature has been attributed to the exchange of water molecules from the interlayer void inside cement hydrates nano-grains and gel pores[51] similar to what is happening in clay that also exhibits low pressure hysteresis[52–54]. Specifically, calcium clay exhibits smaller residual swelling than sodium clay due to stronger ion-ion correlation forces (ICF)[55]. Calcium hydrate layers inside the nano-grains are 4-5 times more charged than these in clay montmorillonite[56]. This corresponds to very large attractive electrostatic ICFs that probably do not allow swelling by contrast to clay. There is a long standing debate in the literature that started sixty years ago with the seminal works of Feldman et al[39] and Hagymassy et al[48] showing opposite conclusions on the existence on the low pressure water adsorption/desorption isotherm at room temperature. More recently Saeidpour et al[33] using dynamic vapor sorption have shown the presence of a low pressure hysteresis. Along the same line, Baroghel-Bouny showed that water adsorption/desorption at 44 °C does not exhibit low pressure hysteresis, indicating that this is likely a kinetic issue due to deficient equilibrium conditions[49]. In this work, we are focusing only on the high pressure capillary effect ($h > 30\%$) and its poromechanical consequences and therefore not considering the water exchange between the inside of cement hydrates nano-grains and gel or capillary pores that is said to occur at relative humidity

lower than 30%. We assume no volume change of the cement hydrates nano-grains[33,57].

The reversible part of the simulated adsorption/desorption isotherm curve shown in Fig. 1a corresponds to the build up of a molecular nanometric film of various thicknesses depending on the local surface curvature. We found that meta-stable ink-bottleneck (cavitation) states[44] are at the origin of sorption hysteresis in cement paste as shown in Fig. 1b. The high connectivity of the cement paste pore network and the resulting percolating liquid distribution is naturally obtained in our numerical framework without any ad hoc assumption on water distribution in contrast to the aforementioned pendular/funicular ring models.

Capillary stress— Next, we analyze the fluid distribution in the pore network (Fig. 1b) and calculate the mechanical effect of capillary stress in such a complex porous structure. To calculate the capillary stress at a given μ (or h value), the mean-field lattice gas DFT[36] is written in its continuum limit, which is equivalent to the Cahn-Hilliard phase-field model (see e.g. Eqn 3.18 from Cahn et al[58], Eqn 59 from Bazant[59])

$$\begin{aligned}\Omega = &\int \left(k_B T \left[\rho \ln(\rho) + (1-\rho)\ln(1-\rho)\right] - \mu\rho\right) dv \\ &+ \int \left[\frac{w_{ff}}{2} a^2 (\vec{\nabla}\rho)^2 - \frac{w_{ff}}{2}\nu\rho^2\right] dv \\ &+ \iint_{\partial V} d\vec{S} \cdot \left(w_{sf}\rho\vec{n} - \frac{w_{ff}}{2} a^2 \rho \vec{\nabla}\rho\right)\end{aligned} \tag{2}$$

where the order parameter $0 < \rho < 1$ here is the normalized liquid density, ∂V represents the liquid-solid boundary, and all symbols are explained after Eqn 1.

Once we have a suitable free energy, we define the capillary stress tensor, first derived by Korteweg[60,61] (see Eqn.4 from Anderson et al[61]),

$$\overleftrightarrow{\boldsymbol{\sigma}} = \left(p_0(\rho) - \frac{a^2 w_{ff}}{2}(\vec{\nabla}\rho)^2\right)\overleftrightarrow{\boldsymbol{I}} + a^2 w_{ff}\vec{\nabla}\rho \otimes \vec{\nabla}\rho + \overleftrightarrow{\boldsymbol{\sigma}}_0 \tag{3}$$

and use it to express the stress in terms of only the density profile from the DFT simulations in the porous structure. Here $\overleftrightarrow{\boldsymbol{I}}$ is the identity tensor, $\overleftrightarrow{\boldsymbol{\sigma}}_0$ an arbitrary tensor constant,

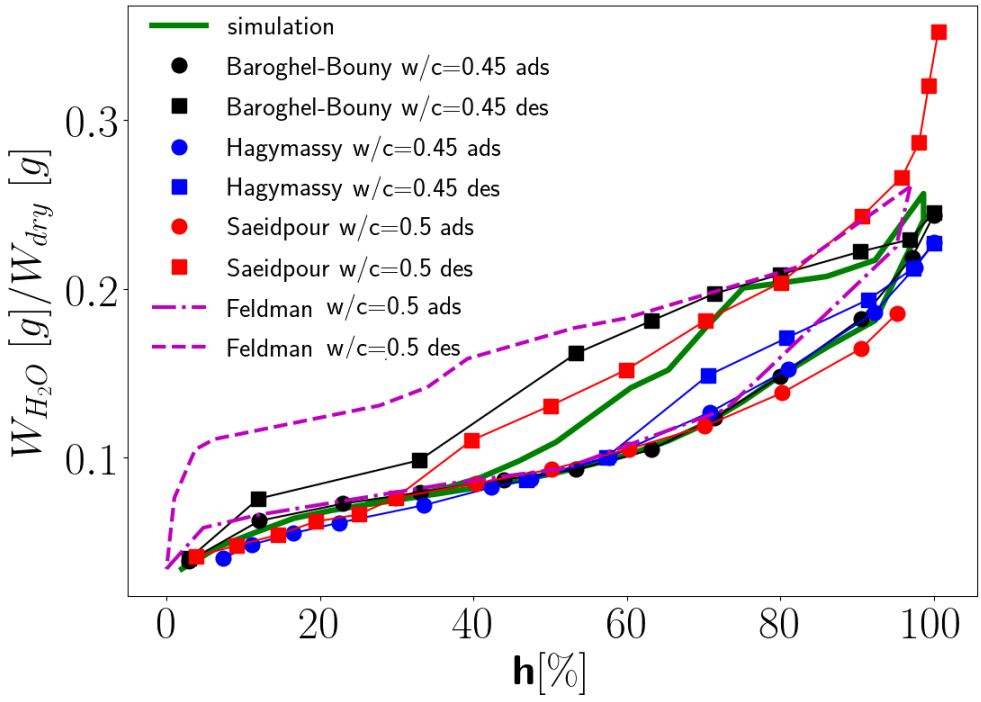

(a)

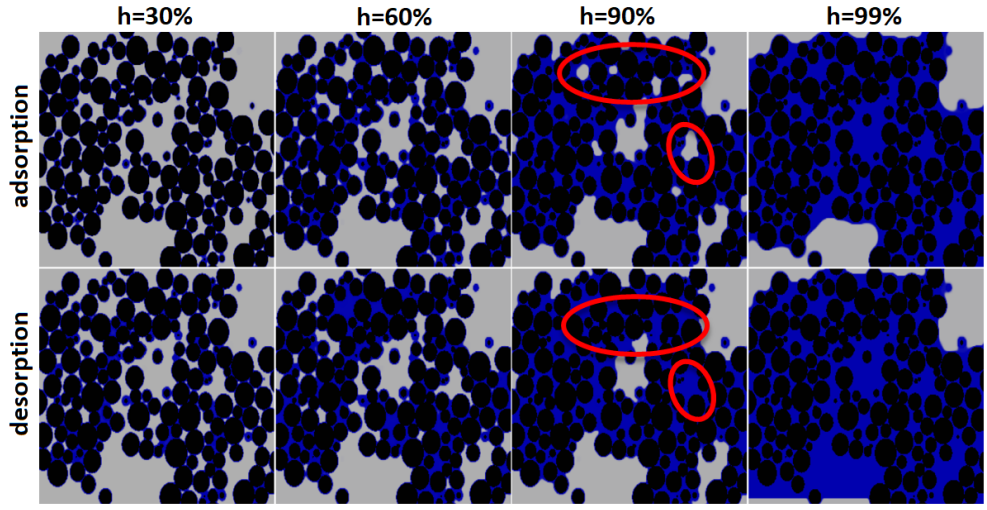

(b)

Figure 1: (a) Simulated water adsorption/desorption isotherm of a mesoscale cement paste model of volume fraction $\eta = 0.52$[35] compared to experimental data.[6,33,48,49] The isotherm is renormalized with respect to the closure point. (b) Cross section of the pore network showing water upon adsorption/desorption. Black—colloidal nano-particles of CSH. Blue—water. Grey—vapor. Ink-bottleneck effect is exemplified by the red-circled areas.

$p_0(\rho) = \mu\rho + \frac{\nu w_{ff}}{2}\rho^2 - k_B T\left[\rho\ln(\rho) + (1-\rho)\ln(1-\rho)\right]$ the asymptotic bulk value of the hydrostatic pressure, and other symbols the same as in Eqn.2 (see derivation for Eqn.3 in SI). In principle, surface forces can be calculated by integrating the normal stress over the solid pore walls, but we find that this procedure leads to large errors for complex geometries.

We thus introduce the second step of our method, which uses Stokes' theorem[62] to deform the contour away from the solid surface and integrate the normal stress over a space-filling tessellation of the microstructure. In this way, equal and opposite forces are applied at each face of the tessellation, perfectly satisfying Newton's third law in the fluid, despite adsorbed fluid density fluctuations on the complex surface geometry. For colloidal or granular systems of convex particles, the most natural choice is the Voronoi tessellation, for which fast algorithms are available, such as the package Voro++[63] used below.

Using the lattice-gas DFT model for water, we first apply the method to the simplest case of two nano-grains at short distance. Fig. 2a shows a stable capillary bridge at appropriate relative humidity. Analytical results are available to describe the capillary force[21,27,64], and most models for wet granular materials rely on this picture of a capillary bridge[65–70]. The simulated capillary force versus humidity is shown in Fig. 2b, in agreement with the solution of Kelvin-Laplace equation[71–73], assuming bulk water surface tension. The forces are simulated on the adsorption branch and thus compared with the analytical solution that has the smaller Kelvin radius (in general the Kelvin equation for a capillary bridge between 2 spheres admits 2 solutions, see SI), augmented by a wetting layer of thickness 0.25 nm.

Fig. 2c shows three spheres nearly in contact to illustrate the challenges posed by any other geometry. At low humidity, the capillary bridge theory still holds and accurately predicts simulation results. However, at high humidity, these bridges coalesce to fill the region between the particles and drastically alters the forces, in a way that only a molecular based approach can capture such as the DFT simulation used here. This is due in part to the liquid-vapor interface that takes a non-convex shape in three dimensions.

Fig. 3 shows the Voronoi tessellation[63] on the 3D heterogeneous porous packing of polydis-

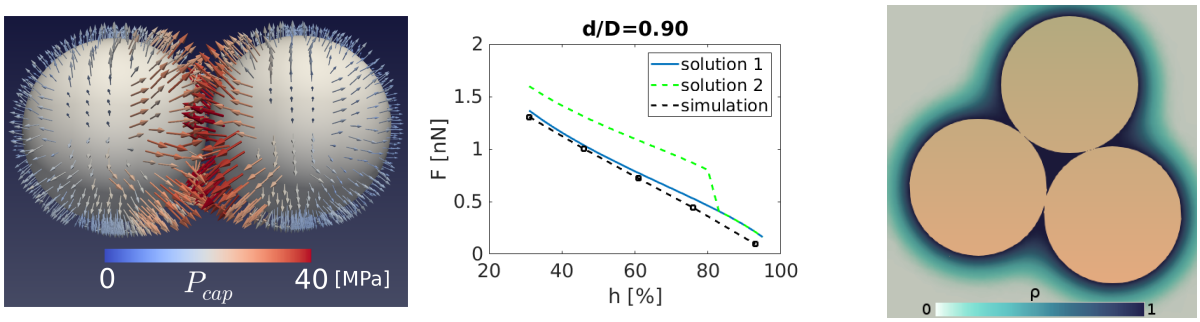

(a) (b) (c)

Figure 2: *Capillary stress*— (a) Simulation of local stresses in the capillary bridge between two spherical colloidal particles of diameter $D = 6$ nm at $h = 30\%$. (b) The total capillary force F on each particle (positive sign for pointing towards the other particle) versus humidity h, compared with the two analytical solutions of Kelvin-Laplace equation (due to the 3D geometry, see SI Eqn. 13) for sphere-center separation $d = 0.9\ D$ (spherical particle diameter $D = 6$ nm) including the surface adsorbed layer. (c) Cross-sectional view of the liquid density ρ filling the region between three touching spherical particles, simulated at $h = 35\%$.

perse cement nano-grains[35] from which stresses can be efficiently and accurately computed. This example demonstrates the capability to predict the stress and deformation of porous materials for any spatial distribution of confined fluid as in the case of equilibrium capillary condensation during drying and wetting processes or in out-of-equilibrium multi-phase flow.

Results

Applying the capillary force on each nano-grain in structural relaxation MD simulations we compute the drying shrinkage of cement paste in quantitative agreement with the experimentally observed volume shrinkage (see Fig. 4). Our findings indicate that capillary forces facilitate macroscopic stress relaxation in granular or colloidal cohesive media with rough and glassy potential energy landscapes and having an abundance of meta-stable states.

Reactive heterogeneous materials such as cement contain residual stresses due to the out-of-equilibrium solidification process[74–76]. The cement paste structure analyzed here has accumulated tensile eigen-stresses of -47 MPa due to the out-of-equilibrium precipitation of nano-grains[47,77]. We refer to this structure as "hardened" cement paste. Then the eigenstress

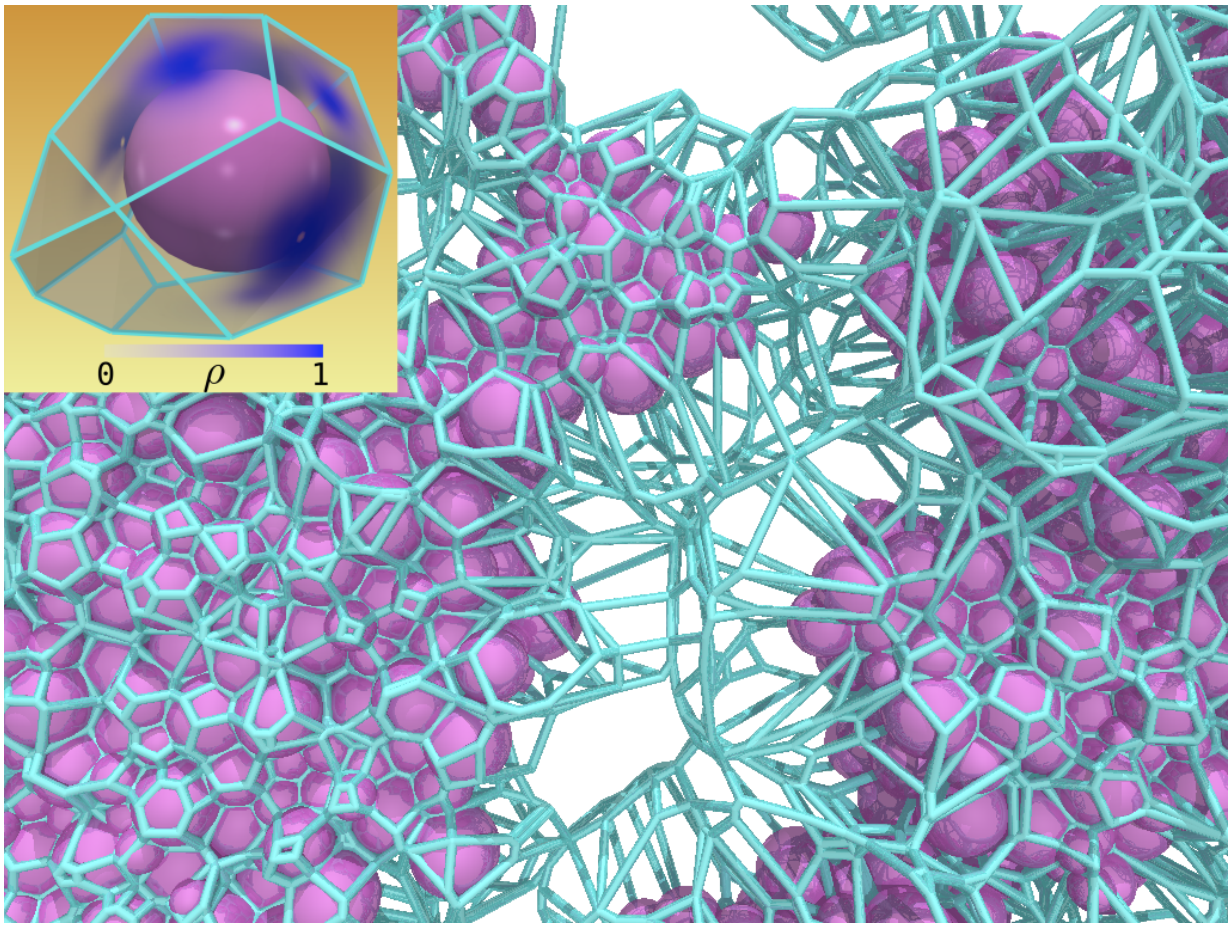

Figure 3: Slice of a polydisperse heterogeneous sphere packing, showing the Voronoi tessellation used to calculate capillary stresses, in the colloidal cement paste[35]. The inset shows adsorbed fluid density profile (blue) on the faces of the Voronoi cell for a single grain at $h = 30\%$.

was relaxed (less than 10 kPa) using energy minimization in NPT conditions (see SI). The relaxed cement paste structure is named "aged".

Figure 4a shows how capillary forces influence the shrinkage strain of "hardened" and "aged" cement paste. In a series of MD structural relaxation simulations, capillary forces calculated at corresponding relative humidities h were applied on the nano-grains as force vectors in addition to the cohesive interactions of cement hydrates nano-grains (see SI). The "aged" model exhibits shrinkage only due to capillary effect whereas the "hardened" sample shrinks under the combined action of tensile eigen-stresses and capillary forces. In the "aged" sample, the pure capillary effect decreases with increasing humidity, and the predicted strain is in agreement with experiment[39] for $h > 30\%$ on the first drying cycle. In contrast, the "hardened" sample shrinks more than the "aged" one and with the opposite trend: the amount of shrinkage strain increases upon increasing humidity. This counter-intuitive behaviour was also observed in short-term cycling h cement experiments after long-term curing of the cement paste samples under a series of constant relative humidities[42]. Our relaxation scheme with capillary forces at constant h coupled to nano-grains cohesive interactions would correspond to the long-term curing conditions of the experiments in Ref.[42]. It is interesting to note that our relative strain results are in surprisingly good agreement with the total strain measurement of Fig. 4 in Ref.[42].

In Fig. 4b, we investigated stress relaxation under constant volume constraint. Minimal residual stresses are observed in the "aged" paste for all humidities. Residual stresses in the "hardened" paste were relaxed to -30 MPa at $h = 30\%$ (closure point of the hysteresis loop), significantly different than that obtained in dry condition (-44 MPa). Overall, capillary forces help relaxing eigen-stresses with the lowest volume shrinkage. It is remarkable to notice the synergistic effect of capillaries and eigen-stresses, reducing the shrinkage compared to dry or fully saturated conditions.

These results demonstrate that capillary stress at intermediate humidity is an effective mechanism of eigen-stress relaxation developed during setting and therefore beneficial to

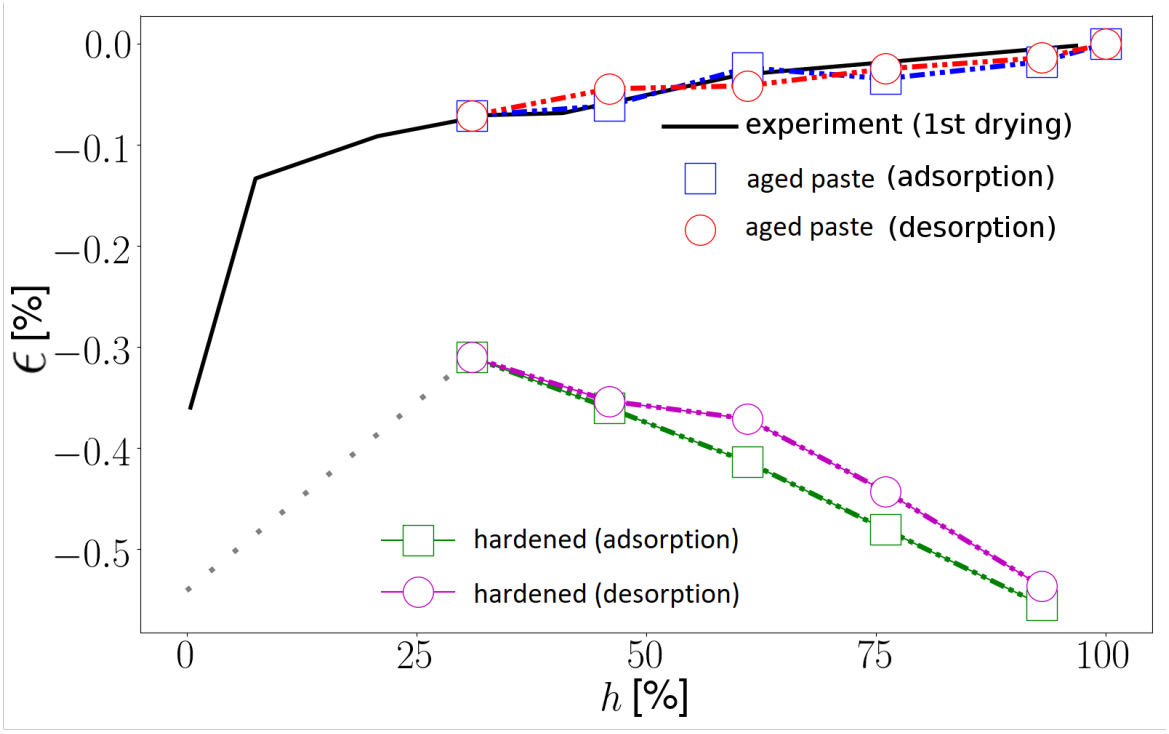

(a)

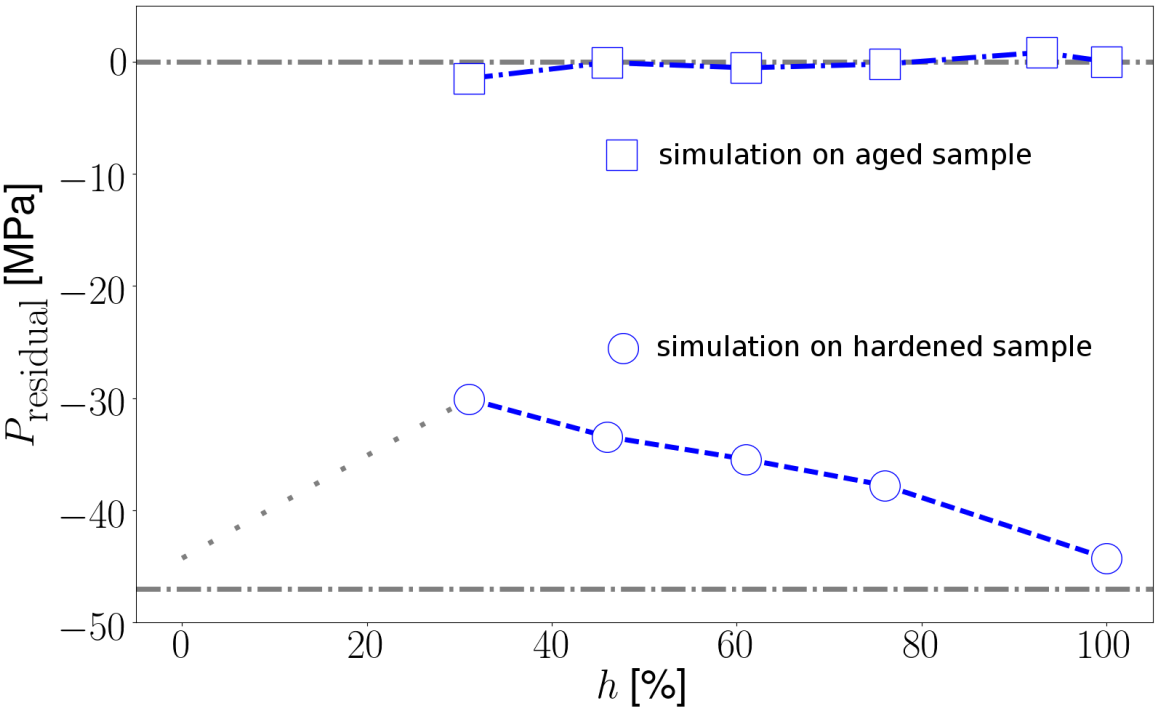

(b)

Figure 4: Stress relaxation of "hardened" and "aged" cement pastes configurations in (a) constant pressure (NPT) and (b) constant volume (NVT) MD simulations under the action of capillary forces. The experimental data are from Ref. [39,51] for cement paste of w/c=0.5

cement durability. Although the magnitude of capillary forces on each nano-grain is small ($\sim$1 nN) compared to the grain-grain interactions ($\sim$10 nN), these forces still have an observable effect at the mesoscale. For materials that are "softer" than cement paste (e.g. wood[78], biopolymers[79]), capillary forces are expected to have even larger aging effects.

Conclusion

In conclusion, we have demonstrated that a mean field lattice DFT approach with suitable molecular scale energy parameters and lattice discretization fineness is able to predict the hysteretic adsorption/desorption isotherm of water in a realistic mesoscale cement paste model further validating this colloidal description of cement hydrates. We further extended this DFT approach to calculate capillary stress from the confined fluid distribution and formulated a general framework to calculate capillary stress in complex porous media, without any assumptions on the pore morphology or topology, across the full range of liquid saturation. Interestingly enough, we found that when combined to the cohesive interactions of the nano-grains, the capillary stress at h 30% actually helps removing the eigen-stress of the cement paste that results from the out-of-equilibrium setting conditions. Our approach is for the first time predicting capillary stress and structural relaxation in cement paste based on statistical physics combined with a realistic mesoscale texture, taking into account fluid-solid coupling explicitly. This is of both theoretical and practical importance due to cement's multi-scale challenging texture and its wide usage in everyday life.

Acknowledgement

This work was supported by the Concrete Sustainability Hub at MIT, CNRS and the A*MIDEX foundation. The authors thank F.-J. Ulm, S. Yip , N. Nadkarni and S. Moeini for useful discussions and C. Rycroft for help with visualization.

Supporting Information Available

1. Phase-field formulation and capillary stress calculation.

2. Numerical simulations: 1) microstructure of cement paste. 2) simulation of adsorption/desorption isotherms. 3) structural relaxation with capillary stress.

This material is available free of charge via the Internet at `http://pubs.acs.org/`.

References

(1) Bocquet, L.; Charlaix, E.; Ciliberto, S.; Crassous, J. Moisture-induced ageing in granular media and the kinetics of capillary condensation. *Nature* **1998**, *396*, 735–737.

(2) Li, K. W.; Hsu, Y.-W.; Chang, W.-R.; Lin, C.-H. Friction measurements on three commonly used floors on a college campus under dry, wet, and sand-covered conditions. *Safety Science* **2007**, *45*, 980–992.

(3) Binggeli, M.; Mate, C. Influence of capillary condensation of water on nanotribology studied by force microscopy. *Applied physics letters* **1994**, *65*, 415–417.

(4) Burdine, N. Relative permeability calculations from pore size distribution data. *Journal of Petroleum Technology* **1953**, *5*, 71–78.

(5) Corey, A. T. The interrelation between gas and oil relative permeabilities. *Producers monthly* **1954**, *19*, 38–41.

(6) Feldman, R. F.; Sereda, P. J. A model for hydrated Portland cement paste as deduced from sorption-length change and mechanical properties. *Materials and structures* **1968**, *1*, 509–520.

(7) Igarashi, S.-i.; Bentur, A.; Kovler, K. Autogenous shrinkage and induced restraining stresses in high-strength concretes. *Cement and Concrete Research* **2000**, *30*, 1701–1707.

(8) Coussy, O. *Mechanics and physics of porous solids*; John Wiley & Sons, 2011.

(9) Singh, K. B.; Tirumkudulu, M. S. Cracking in drying colloidal films. *Physical review letters* **2007**, *98*, 218302.

(10) Routh, A. F. Drying of thin colloidal films. *Reports on Progress in Physics* **2013**, *76*, 046603.

(11) Tirumkudulu, M. S.; Russel, W. B. Cracking in drying latex films. *Langmuir* **2005**, *21*, 4938–4948.

(12) Suh, K. Y.; Lee, H. H. Capillary Force Lithography: Large-Area Patterning, Self-Organization, and Anisotropic Dewetting. *Advanced Functional Materials* **2002**, *12*, 405–413.

(13) Hor, J. L.; Jiang, Y.; Ring, D. J.; Riggleman, R. A.; Turner, K. T.; Lee, D. Nanoporous Polymer-Infiltrated Nanoparticle Films with Uniform or Graded Porosity via Undersaturated Capillary Rise Infiltration. *ACS nano* **2017**, *11*, 3229–3236.

(14) Manohar, N.; Stebe, K. J.; Lee, D. Solvent-Driven Infiltration of Polymer (SIP) into Nanoparticle Packings. *ACS Macro Letters* **2017**, *6*, 1104–1108.

(15) Manoharan, V. N.; Elsesser, M. T.; Pine, D. J. Dense packing and symmetry in small clusters of microspheres. *Science* **2003**, *301*, 483–487.

(16) Schnall-Levin, M.; Lauga, E.; Brenner, M. P. Self-assembly of spherical particles on an evaporating sessile droplet. *Langmuir* **2006**, *22*, 4547–4551.

(17) Lauga, E.; Brenner, M. P. Evaporation-driven assembly of colloidal particles. *Physical review letters* **2004**, *93*, 238301.

(18) Cho, Y.-S.; Yi, G.-R.; Lim, J.-M.; Kim, S.-H.; Manoharan, V. N.; Pine, D. J.; Yang, S.-M. Self-organization of bidisperse colloids in water droplets. *Journal of the American Chemical Society* **2005**, *127*, 15968–15975.

(19) Larson, N. M.; Zok, F. W. fluid flow in deformable porous media: insights from in-situ x-ray computed tomography. *Proceedings of the National Academy of Sciences, (under review)*

(20) Fanale, F.; Cannon, W. Mars: CO2 adsorption and capillary condensation on clays-significance for volatile storage and atmospheric history. *Journal of Geophysical Research: Solid Earth* **1979**, *84*, 8404–8414.

(21) Scholtès, L.; Hicher, P.-Y.; Nicot, F.; Chareyre, B.; Darve, F. On the capillary stress tensor in wet granular materials. *International journal for numerical and analytical methods in geomechanics* **2009**, *33*, 1289–1313.

(22) Wang, K.; Sun, W. Anisotropy of a tensorial Bishop's coefficient for wetted granular materials. *Journal of Engineering Mechanics* **2015**, *143*, B4015004.

(23) Duriez, J.; Wan, R. Stress in wet granular media with interfaces via homogenization and discrete element approaches. *Journal of Engineering Mechanics* **2016**, *142*, 04016099.

(24) Ravikovitch, P. I.; Neimark, A. V. Density functional theory model of adsorption deformation. *Langmuir* **2006**, *22*, 10864–10868.

(25) Jakubov, T. S.; Mainwaring, D. E. Adsorption-induced dimensional changes of solids. *Physical Chemistry Chemical Physics* **2002**, *4*, 5678–5682.

(26) Gor, G. Y.; Neimark, A. V. Adsorption-induced deformation of mesoporous solids. *Langmuir* **2010**, *26*, 13021–13027.

(27) Andrienko, D.; Patrıcio, P.; Vinogradova, O. I. Capillary bridging and long-range attractive forces in a mean-field approach. *The Journal of chemical physics* **2004**, *121*, 4414–4423.

(28) Melnikov, K.; Wittel, F. K.; Herrmann, H. J. Micro-mechanical failure analysis of wet granular matter. *Acta Geotechnica* **2016**, *11*, 539–548.

(29) Melnikov, K.; Mani, R.; Wittel, F. K.; Thielmann, M.; Herrmann, H. J. Grain-scale modeling of arbitrary fluid saturation in random packings. *Physical Review E* **2015**, *92*, 022206.

(30) Gor, G. Y.; Huber, P.; Bernstein, N. Adsorption-induced deformation of nanoporous materials–A review. *Applied Physics Reviews* **2017**, *4*, 011303.

(31) Schappert, K.; Pelster, R. Unexpected sorption-induced deformation of nanoporous glass: Evidence for spatial rearrangement of adsorbed argon. *Langmuir* **2014**, *30*, 14004–14013.

(32) Eriksson, J. C. Thermodynamics of surface phase systems: V. Contribution to the thermodynamics of the solid-gas interface. *Surface Science* **1969**, *14*, 221–246.

(33) Saeidpour, M.; Wadsö, L. Moisture equilibrium of cement based materials containing slag or silica fume and exposed to repeated sorption cycles. *Cement and Concrete Research* **2015**, *69*, 88–95.

(34) Silvestre-Albero, A. M.; Juarez-Galan, J. M.; Silvestre-Albero, J.; Rodríguez-Reinoso, F. Low-pressure hysteresis in adsorption: an artifact? *The Journal of Physical Chemistry C* **2012**, *116*, 16652–16655.

(35) Ioannidou, K.; Krakowiak, K. J.; Bauchy, M.; Hoover, C. G.; Masoero, E.; Yip, S.; Ulm, F.-J.; Levitz, P.; Pellenq, R. J.-M.; Del Gado, E. Mesoscale texture of cement hydrates. *Proceedings of the National Academy of Sciences* **2016**, *113*, 2029–2034.

(36) Kierlik, E.; Monson, P.; Rosinberg, M.; Tarjus, G. Adsorption hysteresis and capillary condensation in disordered porous solids: a density functional study. *Journal of Physics: Condensed Matter* **2002**, *14*, 9295.

(37) Bonnaud, P.; Ji, Q.; Coasne, B.; Pellenq, R.-M.; Van Vliet, K. Thermodynamics of water confined in porous calcium-silicate-hydrates. *Langmuir* **2012**, *28*, 11422–11432.

(38) Pellenq, R. J.-M.; Levitz, P. E. Capillary condensation in a disordered mesoporous medium: a grand canonical Monte Carlo study. *Molecular Physics* **2002**, *100*, 2059–2077.

(39) Feldman, R. Sorption and Length Change, Scanning Isotherms of Methanol and Water on Hydrated Portland Cement. Proc. Fifth Int. Symp. Chem. Cement, Tokyo. 1968.

(40) Parrott, L. The effect of moisture content upon the elasticity of hardened cement paste. *Magazine of concrete research* **1973**, *25*, 17–20.

(41) Scherer, G. W. Drying, shrinkage, and cracking of cementitious materials. *Transport in Porous Media* **2015**, *110*, 311–331.

(42) Maruyama, I.; Igarashi, G.; Nishioka, Y. Bimodal behavior of CSH interpreted from short-term length change and water vapor sorption isotherms of hardened cement paste. *Cement and Concrete Research* **2015**, *73*, 158–168.

(43) Kierlik, E.; Monson, P.; Rosinberg, M.; Sarkisov, L.; Tarjus, G. Capillary condensation in disordered porous materials: Hysteresis versus equilibrium behavior. *Physical review letters* **2001**, *87*, 055701.

(44) Coasne, B.; Galarneau, A.; Pellenq, R. J.; Di Renzo, F. Adsorption, intrusion and freezing in porous silica: the view from the nanoscale. *Chemical Society Reviews* **2013**, *42*, 4141–4171.

(45) Detcheverry, F.; Kierlik, E.; Rosinberg, M.; Tarjus, G. Mechanisms for gas adsorption and desorption in silica aerogels: The effect of temperature. *Langmuir* **2004**, *20*, 8006–8014.

(46) Kierlik, E.; Rosinberg, M.; Tarjus, G.; Viot, P. Equilibrium and out-of-equilibrium (hysteretic) behavior of fluids in disordered porous materials: Theoretical predictions. *Physical Chemistry Chemical Physics* **2001**, *3*, 1201–1206.

(47) Ioannidou, K.; Del Gado, E.; Ulm, F.-J.; Pellenq, R. J.-M. Inhomogeneity in Cement Hydrates: Linking Local Packing to Local Pressure. *Journal of Nanomechanics and Micromechanics* **2017**, *7*, 04017003.

(48) Hagymassy, J.; Odler, I.; Yudenfreund, M.; Skalny, J.; Brunauer, S. Pore structure analysis by water vapor adsorption. III. Analysis of hydrated calcium silicates and portland cements. *Journal of Colloid and Interface Science* **1972**, *38*, 20 – 34.

(49) Baroghel-Bouny, V. Water vapour sorption experiments on hardened cementitious materials: Part I: Essential tool for analysis of hygral behaviour and its relation to pore structure. *Cement and Concrete Research* **2007**, *37*, 414–437.

(50) Naono, H.; Hakuman, M. Analysis of porous texture by means of water vapor adsorption isotherm with particular attention to lower limit of hysteresis loop. *Journal of colloid and interface science* **1993**, *158*, 19–26.

(51) Pinson, M. B.; Masoero, E.; Bonnaud, P. A.; Manzano, H.; Ji, Q.; Yip, S.; Thomas, J. J.; Bazant, M. Z.; Van Vliet, K. J.; Jennings, H. M. Hysteresis from multiscale porosity: Modeling water sorption and shrinkage in cement paste. *Physical Review Applied* **2015**, *3*, 064009.

(52) Cases, J.; Bérend, I.; François, M.; Uriot, J.; Michot, L.; Thomas, F. Mechanism of adsorption and desorption of water vapor by homoionic montmorillonite; 3, The Mg^{2+}, Ca^{2+}, and Ba^{3+} exchanged forms. *Clays and Clay Minerals* **1997**, *45*, 8–22.

(53) Michot, L. J.; Bihannic, I.; Pelletier, M.; Rinnert, E.; Robert, J.-L. Hydration and swelling of synthetic Na-saponites: Influence of layer charge. *American Mineralogist* **2005**, *90*, 166–172.

(54) Tambach, T. J.; Bolhuis, P. G.; Hensen, E. J.; Smit, B. Hysteresis in clay swelling induced by hydrogen bonding: accurate prediction of swelling states. *Langmuir* **2006**, *22*, 1223–1234.

(55) Segad, M.; Jonsson, B.; Åkesson, T.; Cabane, B. Ca/Na montmorillonite: structure, forces and swelling properties. *Langmuir* **2010**, *26*, 5782–5790.

(56) Pellenq, R. J.-M.; Caillol, J. M.; Delville, A. Electrostatic Attraction between Two Charged Surfaces: A (N,V,T) Monte Carlo Simulation. *The Journal of Physical Chemistry B* **1997**, *101*, 8584–8594.

(57) Wu, M.; Johannesson, B.; Geiker, M. A study of the water vapor sorption isotherms of hardened cement pastes: Possible pore structure changes at low relative humidity and the impact of temperature on isotherms. *Cement and Concrete Research* **2014**, *56*, 97 – 105.

(58) Cahn, J. W.; Hilliard, J. E. Free energy of a nonuniform system. I. Interfacial free energy. *The Journal of chemical physics* **1958**, *28*, 258–267.

(59) Bazant, M. Z. Theory of chemical kinetics and charge transfer based on nonequilibrium thermodynamics. *Accounts of chemical research* **2013**, *46*, 1144–1160.

(60) Korteweg, D. J. Sur la forme que prennent les équations du mouvements des fluides si l'on tient compte des forces capillaires causées par des variations de densité considérables mais connues et sur la théorie de la capillarité dans l'hypothèse d'une variation continue de la densité. *Archives Néerlandaises des Sciences exactes et naturelles* **1901**, *6*, 1–24.

(61) Anderson, D. M.; McFadden, G. B.; Wheeler, A. A. Diffuse-interface methods in fluid mechanics. *Annual review of fluid mechanics* **1998**, *30*, 139–165.

(62) Landau, L.; Lifšic, E.; Sykes, J.; Reid, W. *Course of Theoretical Physics*; Teoretičeskaja fizika; Butterworth-Heinenann, 1987.

(63) Rycroft, C. Voro++: A three-dimensional Voronoi cell library in C++. **2009**,

(64) Cheng, T.-L.; Wang, Y. U. Spontaneous formation of stable capillary bridges for firming compact colloidal microstructures in phase separating liquids: a computational study. *Langmuir* **2012**, *28*, 2696–2703.

(65) Kohonen, M. M.; Geromichalos, D.; Scheel, M.; Schier, C.; Herminghaus, S. On capillary bridges in wet granular materials. *Physica A: Statistical Mechanics and its Applications* **2004**, *339*, 7–15.

(66) Scheel, M.; Seemann, R.; Brinkmann, M.; Di Michiel, M.; Sheppard, A.; Herminghaus, S. Liquid distribution and cohesion in wet granular assemblies beyond the capillary bridge regime. *Journal of Physics: Condensed Matter* **2008**, *20*, 494236.

(67) Mitarai, N.; Nori, F. Wet granular materials. *Advances in Physics* **2006**, *55*, 1–45.

(68) Richefeu, V.; El Youssoufi, M. S.; Radjai, F. Shear strength properties of wet granular materials. *Physical Review E* **2006**, *73*, 051304.

(69) Herminghaus, S. Dynamics of wet granular matter. *Advances in Physics* **2005**, *54*, 221–261.

(70) Fournier, Z.; Geromichalos, D.; Herminghaus, S.; Kohonen, M.; Mugele, F.; Scheel, M.; Schulz, M.; Schulz, B.; Schier, C.; Seemann, R. Mechanical properties of wet granular materials. *Journal of Physics: Condensed Matter* **2005**, *17*, S477.

(71) Barrett, E. P.; Joyner, L. G.; Halenda, P. P. The determination of pore volume and area distributions in porous substances. I. Computations from nitrogen isotherms. *Journal of the American Chemical society* **1951**, *73*, 373–380.

(72) Thomson, W. 4. On the equilibrium of vapour at a curved surface of liquid. *Proceedings of the Royal Society of Edinburgh* **1872**, *7*, 63–68.

(73) Stifter, T.; Marti, O.; Bhushan, B. Theoretical investigation of the distance dependence of capillary and van der Waals forces in scanning force microscopy. *Physical Review B* **2000**, *62*, 13667.

(74) Abuhaikal, M. M. A. Expansion and shrinkage of early age cementitious materials under saturated conditions: the role of colloidal eigenstresses. Ph.D. thesis, Massachusetts Institute of Technology, 2016.

(75) Ulm, F.-J.; Pellenq, R. J. Shrinkage Due to Colloidal Force Interactions. *Proceedings of the CONCREEP10 conference, Vienna, Austria, Sept 2015, Ed. Hellmich et al, ASCE Pub.* **2015**, 13–16.

(76) Abuhaikal, M.; Ioannidou, K.; Petersen, T.; Pellenq, R. J.-M.; Ulm, F.-J. Le Châtelier's conjecture: Measurement of colloidal eigenstresses in chemically reactive materials. *Journal of the Mechanics and Physics of Solids* **2018**, *112*, 334–344.

(77) Ioannidou, K.; Pellenq, R. J.-M.; Del Gado, E. Controlling local packing and growth in calcium–silicate–hydrate gels. *Soft Matter* **2014**, *10*, 1121–1133.

(78) Patera, A.; Derome, D.; Griffa, M.; Carmeliet, J. Hysteresis in swelling and in sorption of wood tissue. *Journal of structural biology* **2013**, *182*, 226–234.

(79) Kulasinski, K.; Guyer, R.; Keten, S.; Derome, D.; Carmeliet, J. Impact of moisture adsorption on structure and physical properties of amorphous biopolymers. *Macromolecules* **2015**, *48*, 2793–2800.

Graphical TOC Entry